Magyar Állami Eötvös Loránd Geofizikai Intézet
GEOFIZIKAI KÖZLEMÉNYEK
XIX. kötet, 3—4. szám

ANALYSIS OF CODAS OF SHALLOW-FOCUS EARTHQUAKES

E. BISZTRICSÁNY*

BISZTRICSÁNY EDE

SEKÉLYFÉSZKŰ FÖLDRENGÉSEK FELÜLETI HULLÁM-KÓDÁJÁNAK VIZSGÁLATA

A földrengések felületi hullámainak időtartama főleg a mérettől függ, a távolság csak kevéssé befolyásolja (BISZTRICSÁNY, 1958). A felületi hullámok tartamának nagy része egy közel azonos amplitúdójú hullámszakasz, az úgynevezett *kóda*. AKI japán kutatónak (1969) a kóda eredetére adott magyarázata hullámszórók segítségével értelmezi a felületi hullámok időtartamának csak mérettől való függését az epicentrum közelében.

Feltételezzük, hogy a szórók széles frekvenciasávú kényszererőként rezgésre gerjesztik a Föld felső részét, amely a gerjesztés tartama alatt váltakozó vastagságú lemezként, rá jellemző periódussal végzi rezgéseit. Ez a rezgés a felületi hullámok kis abszorpciós együtthatója miatt közel azonos időtartammal terjed. Ezért az észlelt kódák periódusait elsősorban az átfutott rétegek saját periódusai határozzák meg. Ezek pedig nem függenek a távolságtól.

5°—50° epicentrumtávolságból származó kódahullámok 1000 adatának felhasználásával periódusgyakorisági görbét szerkesztettünk.

Ezen három jól megkülönböztethető gyakorisági maximumot találunk: 5,6—6,5, 7,6—8,5 és 9,6—10,5 sec-nál. A kódák a föld felszínén μ nagyságrendű függőleges elmozdulást hoznak létre. Ha ezeket az ún. föld-amplitúdókat a periódusok függvényében vizsgáljuk, akkor — a legkisebb négyzetek módszerével — a következő egyenletet kapjuk:

$$T = 4{,}28\, Z - 0{,}47\, Z^2 + 1{,}83, \tag{1}$$

ahol T a kódák periódusa, Z pedig az amplitúdója.

HARDTWIG (1962) mikroszeizmikus talajnyugtalanságra alkalmazott módszerét követve a gyakorisági maximumok helyére az (1) egyenletből T, Z sorozatot számítottunk. Ezekből egymáshoz közel eső T, T' és Z, Z' párokat választottunk ki, amelyeket behelyettesítettünk a Rayleigh-hullámokra levezethető

$$z_0 = \frac{TT' \ln \dfrac{Z'}{Z}}{(T' - T)0{,}772}.$$

* ELTE-MTA Seismological Observatory, Budapest.
Manuscript received: 29, 12, 1969.

egyenletbe, ahol z_0 a réteg vastagsága. A következő értékeket kaptuk:

ΔT	z_0 (km)
5,6— 6,6	13,2
7,5— 8,7	18,4
9,4—10,7	29,6

A három adat bármelyike korrelálható a Kárpát-medence kéregszerkezetének valamely lényeges szintjével, amelyeket szeizmikus mélyszondázással határoztak meg. Az első adat értelmezése bizonytalan, a második valószínűleg a Conrad határfelületig terjedő kéreglemez vastagsága; a harmadik adat pedig valószínűleg a Moho határfelületig terjedő lemeznek, vagyis magának a földkéregnek a (maximális) vastagsága.

Mind a modellkísérletek, mind pedig a sekély fészkű rengések kódájának vizsgálatai alátámasztják, hogy a kódák laza csatolású lemezek — szinte — szabad rezgésének foghatók fel.

Э. БИСТРИЧАНЬ

ИЗУЧЕНИЕ ПОВЕРХНОСТНЫХ ВОЛН-КОД, НАБЛЮДАЕМЫХ ПРИ НЕГЛУБОКОФОКУСНЫХ ЗЕМЛЕТРЯСЕНИЯХ

Продолжительность поверхностных волн землетрясения зависит, в основном, от размера, причем расстояние незначительно влияет на нее (*Бистричань*, 1958). Большая часть продолжительности поверхностных волн представлена отрезком волны почти аналогичной амплитуды, так называемой *кодой*. По соображениям японского исследователя *Аки* (1969) о природе коды, зависимость продолжительности поверхностных волн только от размеров объясняется наличием в близи эпицентра рассеивателей волн.

Предполагается, что рассеиватели, как принудительные силы широкого частотного диапазона, заставляют верхнюю часть Земли выполнять вибрации. Эти вибрации имеют периоды, характерные для изменяющейся мощности мантии. В связи с низким значением коэффициента поглощения поверхностных волн, эти колебания распространяются с почти одинаковой продолжительностью. Поэтому периоды наблюдаемых код определяются, прежде всего, собственными периодами пройденных пластов, а последние не зависят от расстояния.

С использованием 1000 данных о волнахкодах, полученных для эпицентральных расстояний 5°—50°, была составлена кривая повторяемости периодов. На этой кривой выдеяются три хорошо выраженных максимума повторяемости со временами 5,6—6,5; 7,6—8,5 и 9,6—10,5 сек. На поверхности земли коды вызывают вертикальное смещение в размере порядка первых единиц микрона. Если изучать эти так называемые амплитуды Земли в зависимости от периодов, то по методу наименьших квадратов получается следующее уравнение:

$$T = 4{,}28Z - 0{,}47Z^2 + 1{,}83, \qquad (1)$$

где T — периоды код и Z — их амплитуда.

С применением метода *Хардтвига* (1962) для определения микросейсм, для максимумов повторяемости были подсчитаны ряды T, Z по уравнению (1). Из этих рядов выбирались близкие друг к другу пары T, T′ и Z, Z′, которые подставлялись в уравнение для волн Релея

$$z_0 = \frac{T.T' \ln \frac{Z'}{Z}}{(T' - T)\, 0{,}772},$$

где Z_0 — мощность слоя. Были получены следующие величины:

ΔT	z_0 (км)
5,6—6,6	13,2
7,5—8,7	18,4
9,4—10,7	29,6

Каждая из указанных величин коррелируется одним из основных горизонтов земной коры Карпатского Бассейна, определенных по данным ГСЗ. Первая величина интерпретируется неоднозначно, вторая соответствует, по всей вероятности, мощности слоя коры до поверхности Конрада, а третья величина — по всей вероятности, мощности слоя до поверхности Мохоровичича, т. е. (максимальной) мощности самой коры.

Как модельные исследования, так и изучение коды неглубокофокусных землетрясений подтверждают, что коды могут рассматриваться как почти свободные колебания слабо связанных между собой плит (слоев).

Introduction

As referred to earlier (BISZTRICSÁNY, 1958 a, b), the magnitude of shallow-focus earthquakes can be correlated not only to the amplitudes of different wave-types but also to the duration of the surface-waves. The interrelation is expressed in the following formula

$$M = a \log t + b\Delta^\circ + c, \tag{1}$$

where M is the magnitude, t is the duration in minutes, Δ° is the epicentral distance in degrees.

The same formula, as expressed for the Wiechert-seismograph (Budapest):

$$M = 2{,}12 \log t + 0{,}007\,\Delta^\circ + 2{,}66. \tag{1a}$$

Under the term: last vibrations in both equations, the train of trailing last waves, recorded by a seismograph of certain performance and magnification, are meant, obviously differring from the actual termination of the surface waves. The last vibrations, sometimes, scarcely differ from microseisms. Equation (1), however, is valid for every shallow-focus earthquake, at least in the general, one might say, statistical, sense of the word.

The parameters of a recorded surface wave depend on the mechanism of the release and travel, on the structural (furthermore, geotectonical) conditions between the focus and the recording station, and on the instrumental characteristics of the recording seismograph.

The forthcoming analysis is based on records of a seismograph of very small distortion, described later.

Equation (1a) clearly shows that the coefficient of Δ° is rather small. Similar formulas have been obtained elsewhere (SOLOVIEV, 1965; TSUMURA, 1967), too. They were utilized, by neglecting the term Δ°, for magnitude-determination of near earthquakes.

Recent research has completed the above-mentioned advantage by directing attention to the hitherto unexplained last vibrations: the so-called *coda*, which represents, even if regarding its duration, a significant section of surface waves.

Surface waves have, as it is well known, two essential components: Love-waves and Rayleigh-waves (i. e. their modes). Theoretically, however, their existence could be explained within a short interval (duration) only, although they have a long, distance-independent attenuation time. For this phenomenon no satisfactory explanation has been offered so far.

The magnitude of the 1956 Budapest (Dunaharaszti) earthquake was, according to the records of the Krumbach-seismograph of the Budapest Ob-

servatory, M = 5,6. The time-span of its surface wave proved to be abt. 20 min., consequently the velocity of its trailing waves never reached even as high as 20 m/sec.

Referring to Equ. (1a), when M = 6,5, the time-span of surface waves is abt. 60 min, and their velocity is 5—6 m/sec. Thus, with increasing magnitude, the velocity of trailing waves decreases. And, since, at the same time, their duration shows an altogether very small reduction with distance, the coda-concept had to be introduced into the interpretation, requiring research to trace the generation and travel of coda.

Conditions of coda-generation

According to the well-known theoretical assumption, surface waves (i. e. their modes) are generated by constructive interferences of body waves. The body waves, responsible for the generation of surface waves, travel either with total-reflection (if so, with slight energy-loss) or with a so-called "leaking" reflection (if so, with greater energy-loss). In the very nearby surroundings of the epicenter, total reflection can occur on the interface between the topmost sedimentary complex and the underlying formation of higher elasticity.

Consequently, energy will rapidly leave the epicenter's vicinity. This rapid energy-loss is not revealed by any record. The existence of the coda cannot be verified in this way.

With regard to the epicenter's surroundings Aki (1969) gave explanation for the length of coda. He assumed that codas are scattered waves on records of local shocks observed with short-period seismographs, arisen in consequence of the heterogeneity of the near-surface geology. In other words: the coda, this elongated, slightly vibrating section of a surface wave, is generated by scattering, diffraction, reflection of radiated waves on protruding objects of an interface. The coda is nothing else than a "time-stretch" of waves arriving at the location of recording, from various directions and various distances.

In the following discussion, it will be assumed that these scattered waves exert a wide-band force on the unequally thick rock-slabs of the Globe, exciting and forcing them to vibration. The period of these vibrations depends on the thickness and physical properties of the rock-slabs (henceforth sometimes: *layers*, for short) and on the size of the source-area.

If so, surface waves could be regarded as plate-vibrations as well. In the following, a close examination will be given, whether in the surface wave groups of a record, the properties of plate-vibrations can or cannot be recognized.

Dispersion analysis with the aspect of plate-vibration

In another paper (Bisztricsány, 1970) the surface waves of an Atlantic quake of the following parameters were analyzed: $\varphi = 1{,}65\ N$, $\lambda = 15{,}5\ W$, $H = 08\ 01\ 33{,}8$, $M = 6\ 3/4$. On the record of a vertical seismograph eight narrow-band mathematical filters were applied with the following band-passes:

$$14 \leq T \leq 16, \quad 16 \leq T \leq 18, \quad 18 \leq T \leq 20, \quad 20 \leq T \leq 22$$
$$22 \leq T \leq 24, \quad 24 \leq T \leq 26, \quad 26 \leq T \leq 28, \quad 28 \leq T \leq 30$$

The shape of vibrations obtained in this way (Fig. 1) is very similar to the well-known figure of the forced vibrations of definite duration (Fig. 2).

Before going on with the analysis of the results of Fig. 1, let us give a consideration to the vibration-characteristics of a plane-parallel plate.

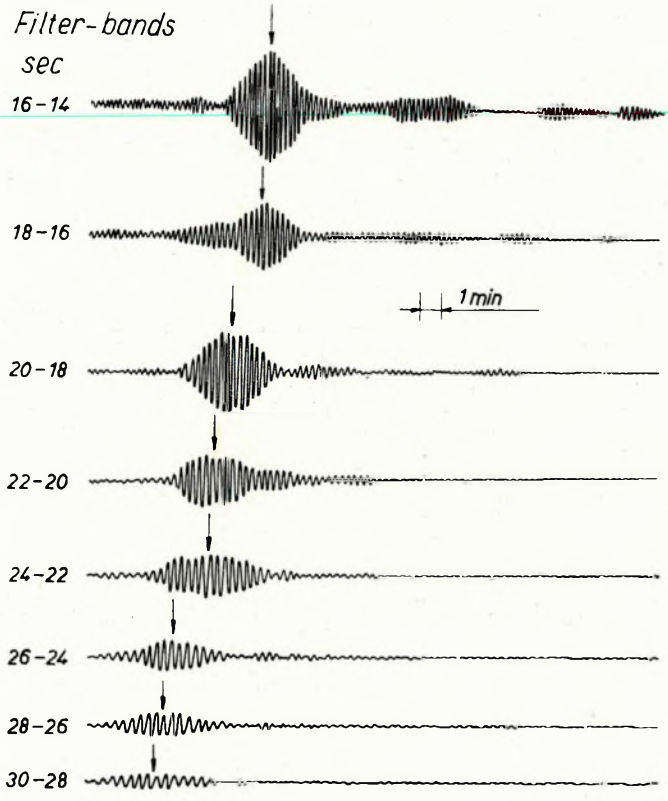

Fig. 1 Narrow-band mathematical filtering on a record
1. ábra Szűksávú matematikai szűrőkön átengedett szeizmogramok
Рис. 1. Сейсмограммы, полученные после применения узкополосных математических фильтров

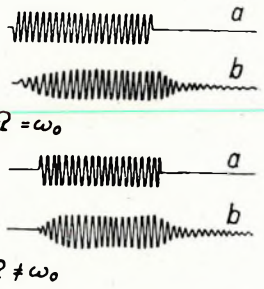

Fig. 2 Forced vibrations (after Trendelenburg)
a) force
b) vibration
2. ábra Kényszerrezgések (Trendelenburg nyomán)
a) kényszerítő erő
b) kényszer rezgés
Рис. 2. Принудительные колебания (по Тренделенбургу)
а) принудительная сила
б) принудительные колебания

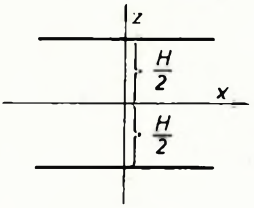

Рис. 3.
Fig. 3
3. ábra

The vibration-characteristics of infinite, homogeneous plane-parallel plates were mathematically established by LAMB (1917).

Let the plane defined by coordinates x, y coincide with plane $z=0$ (Fig. 3), where z points upward, and the limiting planes of the plate of a thickness H be

$$z = \pm\frac{H}{2}.$$

The components u and w of the displacement-vector should satisfy the following equations:

$$\varrho \frac{\partial^2 u}{\partial t^2} = (\lambda + \mu) \frac{\partial \Theta}{\partial x} + \mu \frac{\partial u}{\partial x},$$

$$\varrho \frac{\partial^2 w}{\partial t^2} = (\lambda + \mu) \frac{\partial \Theta}{\partial z} + \mu \frac{\partial w}{\partial z},$$

where ϱ is the density, t is the time, λ and μ are the Lamé-constants. Introducing Φ and ψ scalar and vectorial potentials in the

$$u = \frac{\partial \Phi}{\partial x} + \frac{\partial \psi}{\partial z}; \qquad w = \frac{\partial \Phi}{\partial z} - \frac{\partial \psi}{\partial x}$$

way, these satisfy the Equations

$$\frac{\partial^2 \Phi}{\partial t^2} = V^2 \Delta \Phi \qquad \text{and} \qquad \frac{\partial^2 \psi}{\partial t^2} = v^2 \Delta \psi$$

if

$$V = \sqrt{\frac{\lambda + 2\mu}{\varrho}} \qquad v = \sqrt{\frac{\mu}{\varrho}}.$$

Since our endeavour is to describe surface waves of a plate, functions Φ and ψ should be formulated accordingly:

$$\Phi = (A\ ch\ qz + B\ sh\ qz) e^{ik(x - ct)}$$

$$\psi = (C\ ch\ rz + D\ sh\ rz) e^{ik(x - ct)}$$

Taking the stress limiting conditions $p_{xz} = 0$ and $p_{zz} = 0$ on the defined limiting planes $z = \pm \frac{H}{2}$ into consideration, period-equations

$$\frac{\operatorname{tgh} \frac{H}{2} r}{\operatorname{tgh} \frac{H}{2} q} = \frac{4qr}{k^2 m^2}$$

or

$$\frac{\operatorname{tgh} \frac{H}{2} q}{\operatorname{tgh} \frac{H}{2} r} = \frac{4qr}{k^2 m^2}$$

are obtained, where $m = 2 - \frac{c^2}{v^2}$. These equations offer a relation for plate-thickness H, for k, and consequently for wave-length L.

Introducing the terms

$$\frac{H}{L}=\xi, \quad \frac{c}{v}=\eta \quad \text{and} \quad \frac{kH}{2}=\frac{\pi H}{L}=\pi\xi$$

and $\frac{v}{V}=\varkappa$, further assuming that $\lambda=\mu$, one obtains that $V=v\sqrt{3}$, i.e. $=\frac{1}{\sqrt{3}}$. Substituting the obtained quantities in the period-equations, the latter can be written in the following form:

$$\frac{\operatorname{tgh}\pi\xi\sqrt{1-\eta^2}}{\operatorname{tgh}\pi\xi\sqrt{1-\varkappa^2\xi^2}}=\frac{\sqrt{(1-\eta^2)(1-\varkappa^2\eta^2)}}{\left(1-\frac{1}{2}\eta^2\right)^2}$$

or

$$\frac{\operatorname{tgh}\pi\xi\sqrt{1-\varkappa^2\eta^2}}{\operatorname{tgh}\pi\xi\sqrt{1-\eta^2}}=\frac{\sqrt{(1-\eta^2)(1-\varkappa^2\eta^2)}}{\left(1-\frac{1}{2}\eta^2\right)^2}.$$

The consequence of the bivalence of roots in both equations is that two relative phase-velocities (η) belong to any given wave-length L, the plate-thickness being constant. This means two dispersion-curves. Because of the periodical nature of the *tgh* functions, several modes can be linked to both curves. Thus, it is obvious that having analyzed the plate-waves, dispersion-curves are, in fact, at hand. And now let us turn our attention to the filtered records of Fig. 1.

Dividing the epicentral-distance by the arrival time of the maxima of the arrow-indicated wave-groups of Fig. 1, the velocities of the wave-groups are obtained. Comparing these empirical data with HASKELL'S (1953) theoretical curve and with the empirical data calculated in the usual way, the differences are insignificant (Fig. 4) in either case.

Although the results represented by Figs. 1 and 4 give yet no final justification to regard the surface wave as a plate-vibration, still they are suitable to draw the attention to this possible direction of our investigations.

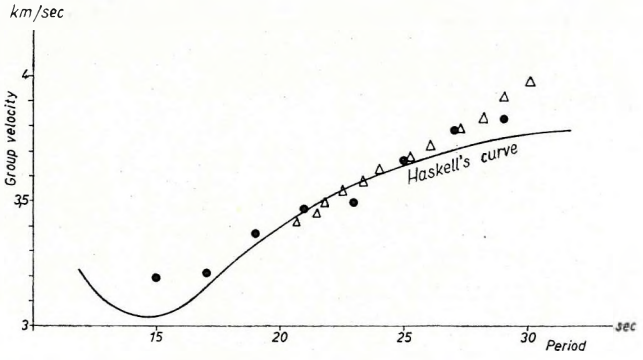

Fig. 4 Dispersion-comparison
● present method
△ traditional method

4. ábra Diszperzió-összehasonlítás
● saját módszer
△ hagyományos módszer

Рис. 4. Сопоставление разбросов
● по собственному методу
△ по стандартному методу

The vibration-process was, in the foregoing, sketched so, that loosely coupled plates vibrated with different resonant-frequencies. If so, there must exist a dominant period, depending on the thickness of the plate, exceeding the rest of the spectrum in recurrence.

In the following items, our investigations of this kind will be summed up, including both ultrasonic model-tests and natural earthquakes.

Ultrasonic model-tests of plate vibrations

It is well known that in infinite, elastic solid media, the velocity of longitudinal waves

$$C_L = \sqrt{\frac{E}{\varrho_0}} \sqrt{\frac{1-\sigma(}{1+\sigma)(1-2\sigma)}}, \tag{2}$$

and that of transverse waves

$$C_T = \sqrt{\frac{E}{\varrho_0}} \sqrt{\frac{1}{2(1+\sigma)}}, \tag{3}$$

where E is Young's modulus, σ is the Poisson-ratio. The value of the former, in solid bodies, varies between $5 \cdot 10^9$ and $5 \cdot 10^{10}$ N/m^2, while that of the latter, between 0,2 and 0,46. Accordingly, velocities vary between 1000 m/sec and 5000 m/sec.

Our first model consists of an aluminum, resp. a synthetic resin plate (disc) in a staggered arrangement (Fig. 5), similar to the model of HEALY and PRESS (1960).

In case of a two-layered plate the equation of motion for a motion in the direction x is

$$\frac{\partial^2 u}{\partial x^2} = \frac{\varrho_1 T_1 + \varrho_2 T_2}{\frac{E}{1-\sigma_1^2} T_1 + \frac{E}{1-\sigma_2^2} T_2} \frac{\partial^2 u}{\partial t^2}. \tag{4}$$

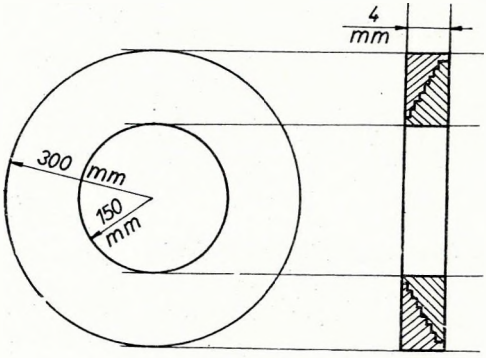

Fig. 5
5. ábra
Рис. 5.

Thus, a T_1, T_2 layered plate's longitudinal velocity C_L is

$$C_L^2 = \frac{\varrho_1 C_{L_1}^2 T_1 + \varrho_2 C_{L_2}^2 T_2}{\varrho_1 T_1 + \varrho_2 T_2} \tag{5}$$

and its transverse velocity C_T is

$$C_T^2 = \frac{\varrho_1 C_{T_1}^2 T_1 + \varrho_2 C_{T_2}^2 T_2}{\varrho_1 T_1 + \varrho_2 T_2} \tag{6}$$

as long as $\lambda \gg T_i$.

The validity of (5) and (6) for the model of Fig. 5. has been experimentally proved (HEALY—PRESS, 1960). This staggered disc-model is, in fact, a multilayered earth-model, where,

proceeding toward the centre of the disc, wave velocity increases according to (5) and (6). Namely, the aluminum-thickness likewise increases in the same direction and wave velocity in aluminum is greater than in synthetic resin (Fig. 6).

One of the aims of model-tests was to establish conditions unknown in Nature (AKI, 1969). In Nature i.e. in the near-surface layers, namely, a great deal of scattering objects are, according to AKI, evenly but irregularly situated, generating a stray wave-field.

In fact, two models were constructed: one with—another without scattering objects, in order to compare the behaviour of both media. When calibrating the realistic earth-model, it had to be taken into consideration that the velocity and reflection index of ultrasonic waves depended on the geometry of the medium traversed.

If a material of an acoustic impedance $\varrho_k c_k$ is embedded in a medium of an acoustic impedance $\varrho_i c_i$ with tight coupling, then, in case of normal incidence (perpendicular traversing) the reflection-index

$$R = \frac{(q^2-1)^2}{(q^2+1)^2 + 4q^2 \operatorname{ctg}^2 (2\pi d/\lambda)}, \qquad (7)$$

where dis the thickness of the embedded object (plate), λ is the wave-length and q is the ratio of the acoustic impedances (that of the embedding medium being in the numerator).

Formula (7) shows that the reflection index depends, aside from q and λ, on d, too. R is at maximum when

$$d = (2n-1)\frac{\lambda}{4} \qquad n = 1, 2, 3, \ldots \qquad (8)$$

and thus one obtains

$$R_{\max} = \left(\frac{q^2-1}{q^2+1}\right)^2.$$

As to the minimum-value of R, it converges toward zero if

$$d = n\lambda/2 \qquad n = 1, 2, 3, \ldots \qquad (9)$$

Equ. (7) gives values of R of synthetic resin embedded in aluminum, in the function of d.

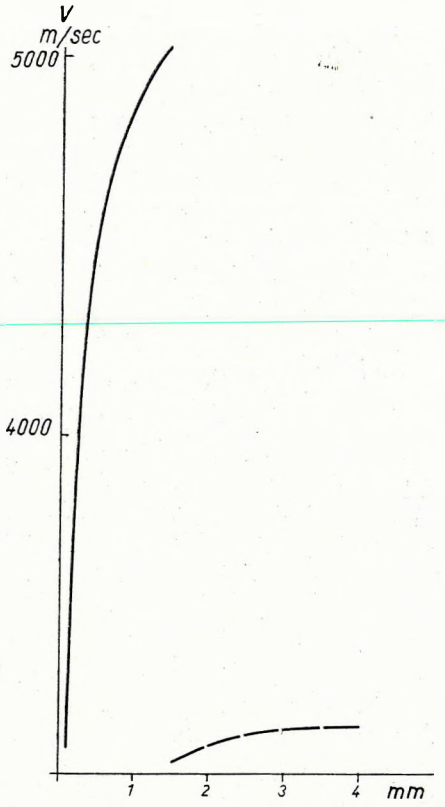

Fig. 6 Wave-velocity in plates in the function of thickness
— aluminum
— synthetic resin

6. ábra Hullámsebesség a lemezvastagság függvényében
— alumínium
— műgyanta

Рис. 6. Зависимость скорости распространения волны от мощности пройденной плиты
— алюминий
— искусственная смола

The ultrasonic seismoscope starts 25 pulses per seconds, i.e. the time-span of the attenuation of waves, as will be shown, is much shorter than the pulse-interval; thus, subsequent pulses don't disturb each other.

The disc-model, however, proved to be unreliable for three reasons.

The first reason was that waves reflected from the inner rim of the disc by too quick reflections might have disturbed the surface wave pattern (although several check-ups were made, the only result was the necessity of another model).

The second reason was that, although the staggered model symbolized the Earth well, and was suitable to trace the travel of body waves, the continuous reflections from the inner boundaries screened the trailing section of surface waves (Figs. 7, 8).

The third, and most serious, reason was that the model allowed exclusively tight coupling between the layers, although, as it will be shown later, one of the most essential factors of our concept is *loose coupling*.

For the above-mentioned reasons, three new models were constructed and laid under test. The new models were square aluminum-sheets of 1 m edge-length. Two of them were 1/2 mm, one of them was 1 mm thick. One of the

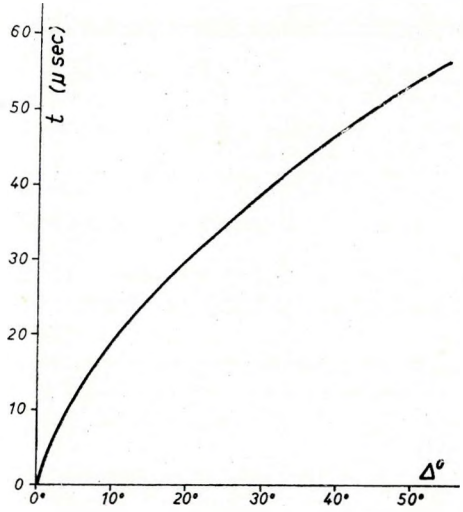

Fig. 7 Travel-time curve for the disc-model

7. ábra A tárcsa-modellre vonatkozó út—idő görbe

Рис. 7. Годограф для дисковой модели

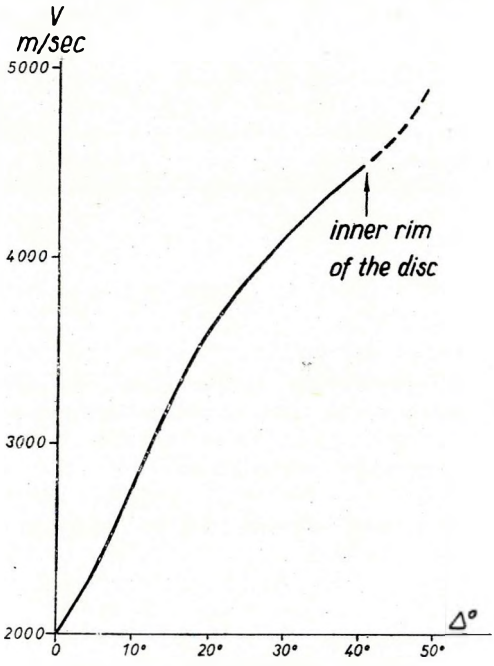

Fig. 8 Apparent velocity vs. distance curve for the disc-model

8. ábra A tárcsa-modellre vonatkozó látszólagos sebesség/út görbe

Рис. 8. Кривая зависимости кажущейся скорости от пройденного пути для дисковой модели

1/2 mm thick sheets was punched by several, irregularly arranged 5×15 mm parallelepiped-holes, inlaid by synthetic resin. A pulse-signal transmitter was placed in the corner of the sheet, the receiver was spaced 10 cm off, diagonally, to exclude the above described screening effect of the rim-waves. The latter, namely, require an interval of at least 400 microseconds, the useful length of our record, on the other hand, remained well below this value. Thus, measurements were made both with a plain (Fig. 9) and with an inlaid sheet (Fig. 10).

When comparing these figures, the different length of the respective wave-patterns is conspicuous. In case of the inlaid plate the attenuation of the wave

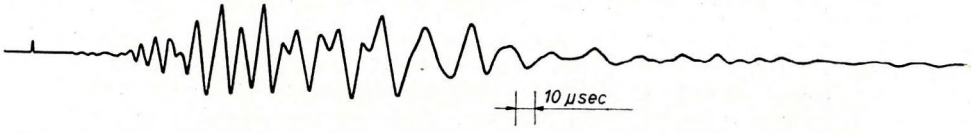

Fig. 9 Shape of vibrations in a 0,5 mm thick aluminum-plate
9. ábra 0,5 mm vastag alumínium lemezben gerjesztett hullámok rezgésképe
Рис. 9. Волновая картина колебаний, возбужденных в алюминиевой плите мощностью 0,5 *мм*

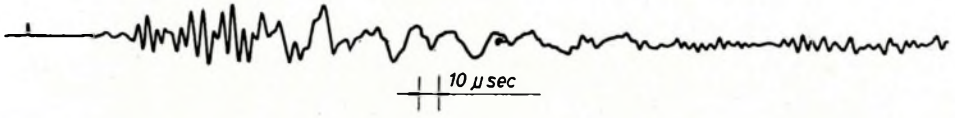

Fig. 10 Shape of vibrations in a 0,5 mm thick aluminum-plate inlaid with scattering objects of synthetic resin
10. ábra 0,5 mm vastag, műgyanta szórókkal megtüzdelt alumínium lemezben gerjesztett hullámok rezgésképe
Рис. 10. Волновая картина колебаний, возбужденных в алюминиевой плите мощностью 0,5 *мм* с рассеивателями из искусственной смолы

is completed by an elongated, high-frequency signal. The maximum amplitude, however, doesn't reach that of the plain plate.

Fig. 11 demonstrates the wave-pattern of the 1 mm thick plate. The maximum amplitude exceeds those of both former ones. The attenuation time-span is somewhat longer than on Fig. 9, but shorter than on Fig. 10. The wave-pattern obtained, bears testimony to the assumption of AKI: the attenuation-section of waves in the inlaid plate (containing scattering objects) is longer, even beside smaller maximum-amplitudes. *Codas can, consequently, really be generated by scattering objects.*

Hence, the next step in the analysis has to involve the examination of dominant periods and characteristic vibration-pattern for individual plates in the following arrangements: different plate-thicknesses; plain versus inlaid plates; single versus coupled duplex; tight coupling versus loose coupling.

Omitting unnecessary details, the most promising arrangement was the following: a 1 mm thick plain aluminum plate overlain by an inlaid 1/2 mm thick plate, with lube-grease inbetween in order to attain loose coupling and an at least partial wave-penetration into the thick bottom-plate without block-

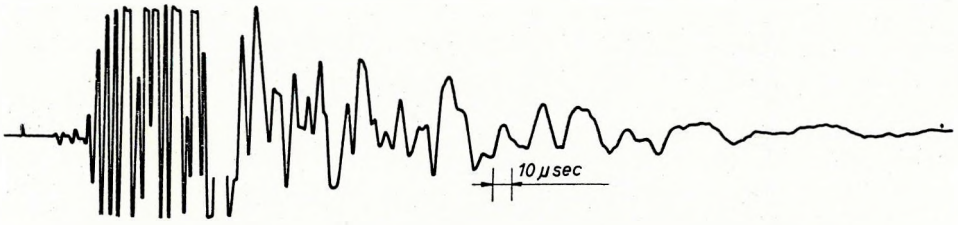

Fig. 11 Shape of vibrations in a 1 mm thick aluminum-plate
11. ábra 1 mm vastag alumínium lemezben gerjesztett hullámok rezgésképe
Рис. 11. Волновая картина колебаний, возбужденных в алюминиевой плите мощностью 1 *мм*

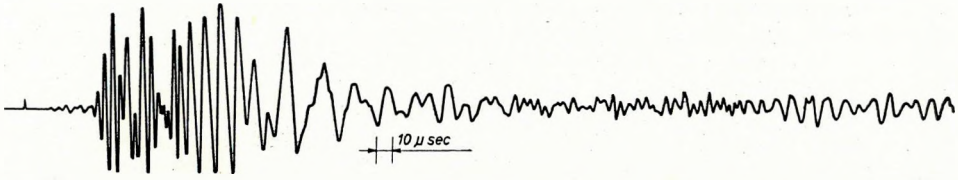

Fig. 12 Shape of vibration for a two-layered plate (duplex), with loose coupling (lube-grease inbetween); top-layer 0,5 mm thick inlaid plate, bottom-layer 1 mm thick plain plate
12. ábra Két lemezben terjedő hullámok rezgésképe; a két lemez között csapágyzsír réteg helyezkedik el: a felső lemez 0,5 mm vastag műgyanta szórókkal megszakított alumínium lemez, az alsó 1 mm vastag sima alumínium lemez
Рис. 12. Волновая картина колебаний, распространяющихся в двух плитах; между плитами располагается слой масла для подшипников; первая плита представлена алюминиевой плитой мощностью 0,5 *мм* с рассеивателями из искусственной смолы, а вторая плита — чистой алюминиевой плитой мощностью 1 *мм*

ing its free vibration (transmitter on the top-plate). The wave-pattern obtained in this way is demonstrated by Fig. 12.

One thing shows instantly up. The maximum amplitude, as compared to that of Fig. 10, increased owing to the thicker plate underneath, and the attenuation-section shows, even to the naked eye, the evenly short-period, long time-span section.

Wave-patterns of Figs. 10, 11 and 12, were turned into period-recurrence spectra (Figs. 13, 14, 15, resp.). Fig. 13 shows a clear maximum at 4,75 microsec, while Fig. 14 shows no such one. Fig. 15, again shows two considerable maxima at 4,75 and 6,75 microsec.

The suggested interpretation is as follows. The waves reflected on the scattering objects in the top-layer (plate) excite both plates (the thin and the thick one equally), and while Fig. 13 reveals a single maximum (one plate vibrated), Fig. 15 must indicate two maxima, since, apparently, the wave-pattern of Fig. 12 is characteristic for both plates.

The large amplitudes indicate, at any rate, that a loose coupling allows vibrations of almost as high an amplitude as a single plate does, although the top-layer's single vibration is weaker than that of the bottom-layer. Coupling, consepuently, brings the top-layer's vibration nearer to the bottom ones, in fact, almost levels them off.

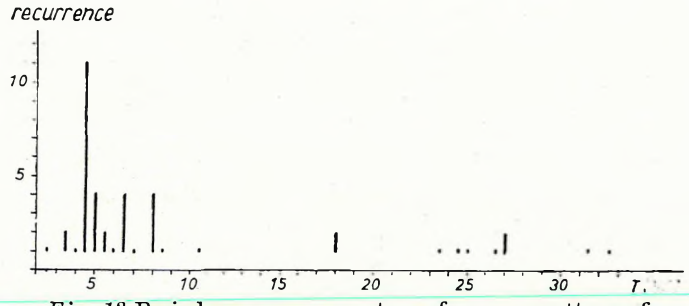

Fig. 13 Period-recurrence spectrum for wave-pattern of Fig. 10

13. ábra A 10. ábra rezgésképéhez tartozó periódusgyakorisági spektrum

Рис. 13. Спектр повторяемости периодов для волновой картины рис. 10.

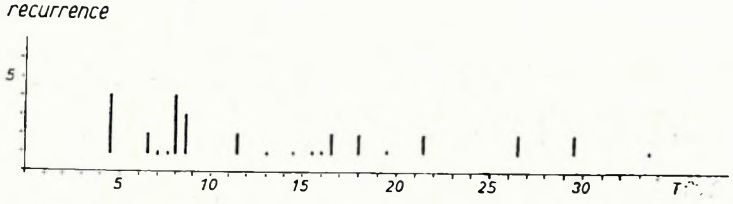

Fig. 14 Period-recurrence spectrum for wave-pattern of Fig. 11

14. ábra A 11. ábrához tartozó periódusgyakorisági spektrum

Рис. 14. Спектр повторяемости периодов для волновой картины рис. 11.

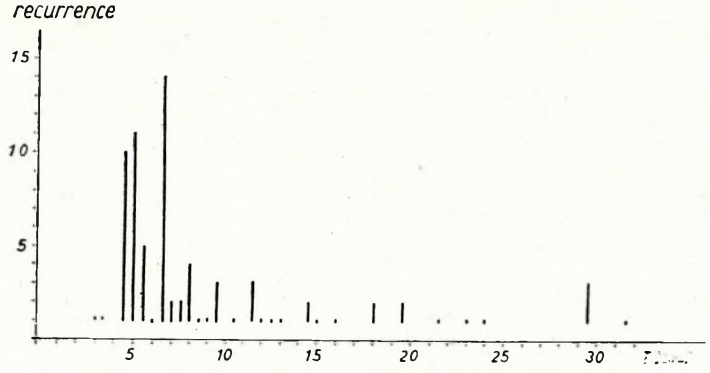

Fig. 15 Period-recurrence spectrum for wave-pattern of Fig. 12

15. ábra A 12. ábrához tartozó periódusgyakorisági spektrum

Рис. 15. Спект повторяемости периодов для волновой картины рис. 12.

The conclusion of the model-tests is that tight coupling (disc-model) blocks dominant-period vibrations of individual layers. Instead, a single period, depending on the material and sum-thickness of the layered disc, will be enhanced. Loosely coupled two plates, however, reveal vibration-characteristics for both plates.

Coda-analysis of shallow-focus earthquakes

Our proper aim is now at hand. An endeavour will be made to interprete, with the model-test background, the surface waves.

The assumption of AKI (1969) concerning the process of coda-generation is fundamentally correct. It must be, however, completed by the results of the model test, namely that the scattering objects excite the loosely coupled plates (layers, or the crust for that matter). The layers start characteristic, eventually resonant-period, vibrations. It will be tried to calculate the thickness of layers from their period-response. And if the values obtained in this way, showed an at least approximate correlation with data collected in another way, the above explanation of coda would not be thought to be jumping at conclusions.

The essential data of the earthquake-analysis are the following. Type of seismograph: Kirnos, vertical. Location: Sopron. Time-interval of recordings: 1968—69. Number of records: 60. Epicentral distance: $5° < \Delta° < 50°$ Parameters of the Kirnos seismograph: pass, between 1 and 10, is near-constant. Magnification: 700-fold. Useful paper-transport velocity (as determined by the pass) 30 mm/min. Actual accuracy of timing: 0,2—0,4 sec.

In order to avoid subjective errors, partly a large volume of data, partly 1 sec period-intervals were used.

When calculating velocity, only epicentral distances were taken into consideration, no other distance-data (e.g. distance of the scattering objects) having been at disposal. Three Figures (16, 17, 18), demonstrating three magnitude-ranges, testify that coda-periods are almost independent of velocity, thus neither regular, nor inverse dispersion must be taken into consideration in the distance range $5° < \Delta° < 50°$.

Before proceeding, it is necessary to examine the dependence of velocity and period of a few waves of the coda, on distance and magnitude. This can be carried out by plotting the average-velocity of the last two-three sizable waves against the distance (with regard to the above-mentioned magnitude-ranges).

Assuming that the relation between velocity and distance can be formulated by

$$v = a\Delta° + b'(M), \tag{10}$$

where $b' = bM + c$, then

$$v = a\Delta° + bM + c \tag{11}$$

can likewise be written.

The constants of Equ. (11) have been tabulated from the data by the method of least squares, arriving at the following equation:

$$v = 0{,}019\ \Delta° - 0{,}32\ M + 2{,}45. \tag{12}$$

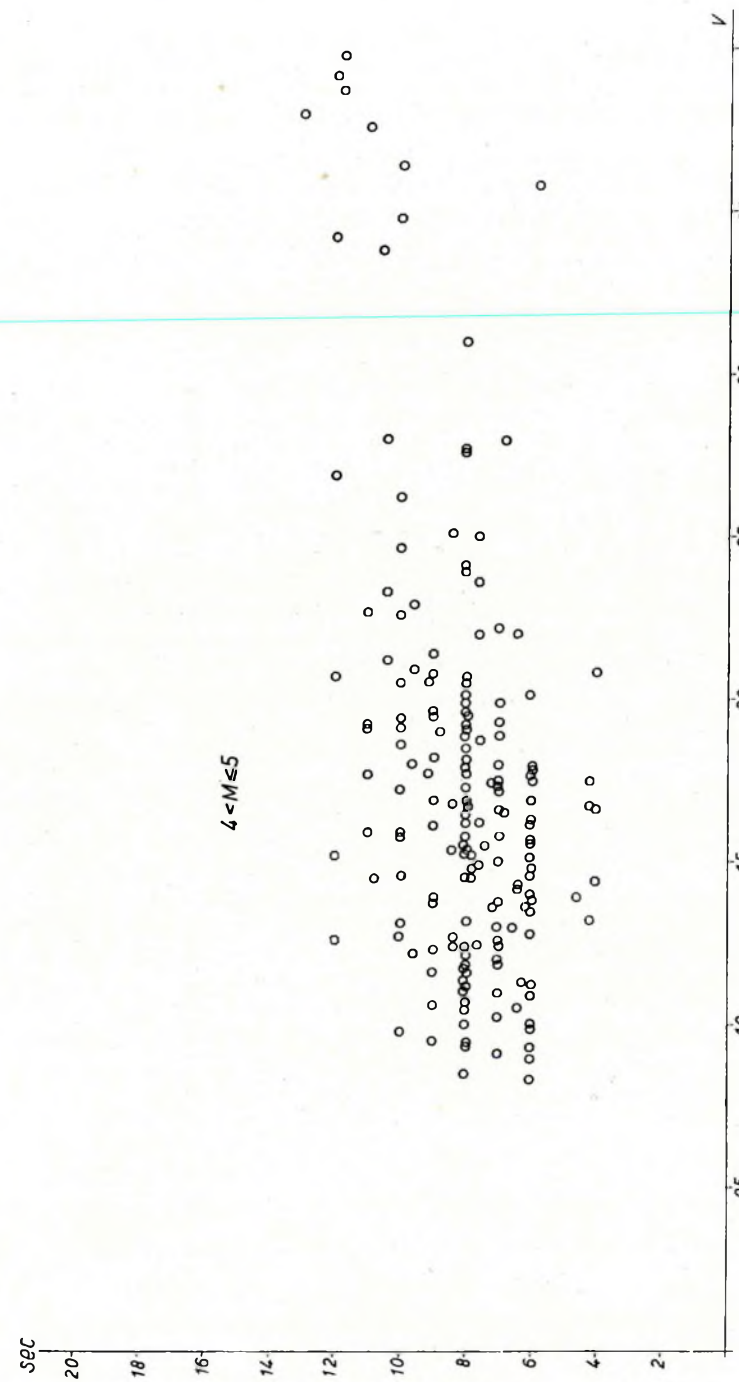

Fig. 16 Velocity of coda-waves of $4 < M \leq 5$ in the function of period

16. ábra $4 < M \leq 5$ méretű rengések kóda-hullámainak sebessége a periódus függvényében

Рис. 16. Зависимость скорости волн-код колебаний размера $4 < M \leqslant 5$ от периода

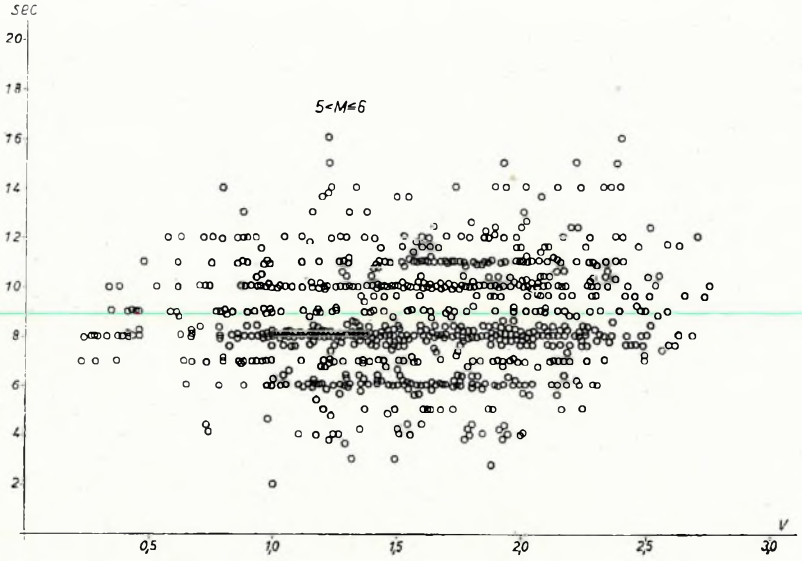

Fig. 17 Velocity of coda-waves of $5{,}1 < M \leq 6$ in the function of period
17. ábra $5{,}1 < M \leq 6$ méretű rengések kóda-hullámainak sebessége a periódusok függvényében
Рис. 17. Зависимость скорости волн-код колебаний размера $5{,}1 < M \leq 6$ от периода

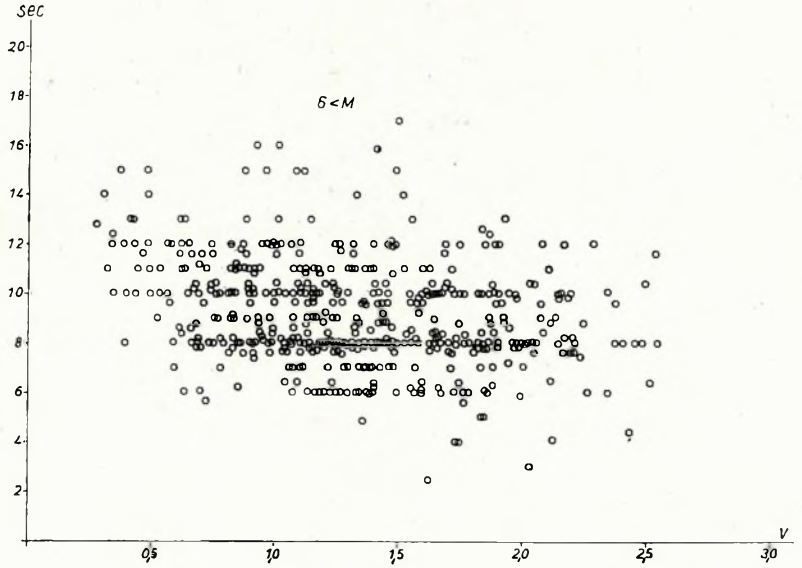

Fig. 18 Velocity of coda-waves of $6 < M$ in the function of period
18. ábra $6 < M$ méretű rengések kóda-hullámainak sebessége a periódusok függvényében
Рис. 18. Зависимость скорости волн-код колебания размера $6 < M$ от периода

The different v values completed with the belonging 0,32 M values and plotted against the distance Δ°, give Fig. 19.

Equ. (12) indicates that v is directly proportional with distance, i.e. to greater epicentral-distances greater velocities belong.

It is worth remarking that (12) is nothing else than another formulation of (1). Namely, rearranging (12), the equation

$$M = -3{,}12v + 0{,}059\,\Delta^\circ + 7{,}65 \tag{13}$$

is obtained.

Equ. (1) states that the time-span of a shallow-focus earthquake depends mainly on magnitude, far less on distance. A longer time-span means that with increasing magnitude, waves of lower velocity can be observed. With other words: small v-s require great M, great v-s require small M values. Equ. (13) likewise contributes to the slight dependence of magnitude on distance.

By calculating the equation with the same considerations for the period (Fig. 20),

$$T = 0{,}043\,\Delta^\circ + 2{,}54\,M - 6{,}07. \tag{14}$$

The coefficient of Δ° is small, in this case, too; neglecting this quantity in case of short distance, from (12) and (14) the following relation is obtained between T and V:

$$0{,}39T + 3{,}12v - 5{,}27 = 0. \tag{15}$$

Putting it into words: to greater periods, lower velocities belong. Since T is one of the last arrivals, Equ. (15) equally informs us about the dispersion and absorption of waves of different periods. The attention must be drawn to the fact that the waves in question are the last two-three waves of a coda, con-

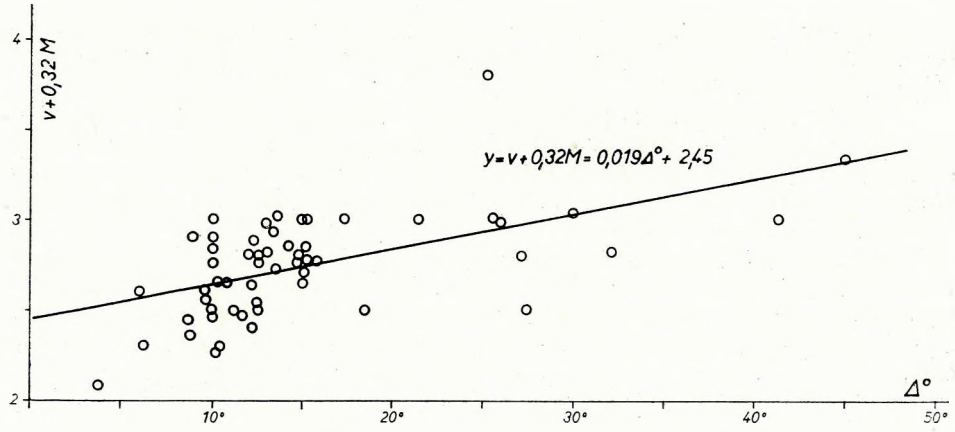

Fig. 19 Velocity of the last waves of a coda in the function of distance
19. ábra A kóda utolsó hullámainak sebessége a távolság függvényében
Рис. 19. Зависимость скорости последних волн коды от расстояния

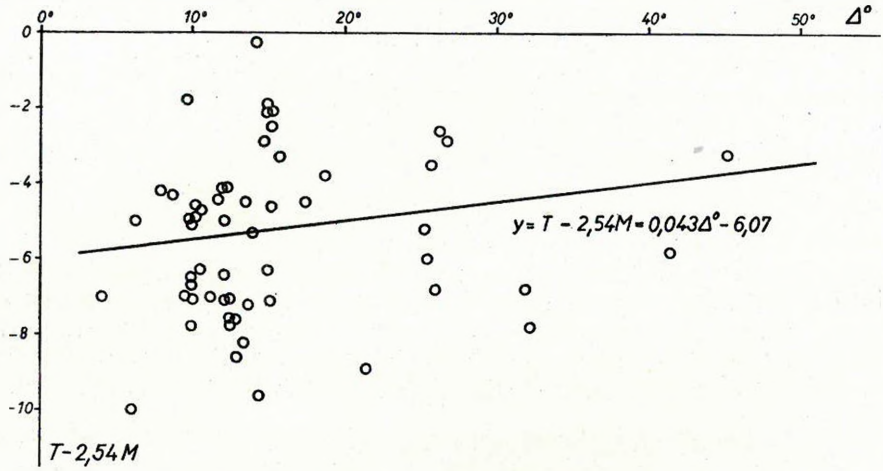

Fig. 20 Distance-dependence of two-there of the last wave-periods of a coda
20. ábra A kóda két-három utolsó hullámának távolságfüggése
Рис. 20. Зависимость двух-трех последних волн коды от расстояния

sequently, Equ. (15) is suitable to determine the disappearence of waves of a certain period, from the attenuation-section.

Equ. (12), (13), (14), (15), however, give information, in this way, about the composition of the termination of coda-waves only. The entire attenuation-section remains unclarified, i.e. the cited four equations are unsuitable to examine the full coda-length.

Layer-thickness determination from coda-waves

Coda-waves involve a significant time-section of surface waves, in fact, the entire part of slightly varying amplitudes. Consequently, the entire length requires close examination.

Referring to the model-tests, first of all a dominant period, characteristic for every coda, is to be searched for. If such a period existed, it could prove that the attenuation-section is nothing else than the natural-frequency response of a plate: in this case the plate being a part of the crust, or the entire layered crust and a part of the mantle-top.

This concept, referring to vibrations of another kind, is not novel at all. HARDTWIG (1962) e.g. stated: "The period-spectra of microseisms reveal extraordinarily sharp recurrence-peaks. Two ways of interpretation are possible: *a)* either forced-vibrations are at hand, when the force must oscillate in identical period, or, *b)* free oscillations of a relatively well defined and delimited body are encountered". HARDTWIG himself refers to earlier authors, and, anyway, it is well known that WIECHERT, as early as in 1907, turned the thought in mind that earthquake-waves and microseisms are innate motions of rock-slabs of vast extension, or of the crust itself. WIECHERT, empirically, assumed that far-earthquakes are, in general, of 17—18 sec period with a wave-velocity

of abt. 3,5 km/sec. The layer-thickness, equal to a half wave-length, can be described by the equation

$$D=\frac{T}{2}\ v=\frac{17{,}5}{2}\cdot 3{,}5\approx 30\ \text{km}.$$

This result fairly coincides with recently measured average crustal thickness.

Wiechert, however, must have considered a short section of a shock of a certain distance. In general, namely, there is empirical proof for this statement, for the periods of surface waves are usually not of 17—18 sec.

Taking the entire attenuation-section into consideration, waves of different periods show different recurrences. The recurrence curves of the above-mentioned shallow-focus earthquakes, as demonstrated on Figs. 16, 17, 18, reveal a more realistic tracing of the phenomenon. According to a preliminary assumption, periods are distance-dependent, therefore period-recurrences are taken by intervals 5°—10°, 10°—20°, 20°—30° and 30°—50°. (It is not necessary to mention that recurrences in each interval were divided by the number of shocks in the same interval, in order to reduce recurrence-curves to a single shock.).

The figures don't reveal the distance-dependence of magnitude as expressed by Equ. (14). It is, however, true that Equ. (14), as mentioned, refers only, to a few last waves of a coda. Except for the interval 5°—10°, where there is one recurrence-peak, two peaks show up in all of the rest of the intervals (Fig. 21).

The recurrence-analysis proved to be so promising that no objection remained against plotting the period-recurrence reduced to one shock, on a single graph, for the entire 5°—50° interval. The two peaks show up, in this way, even more clearly (Fig. 22). With regard, however, to distance-magnitude

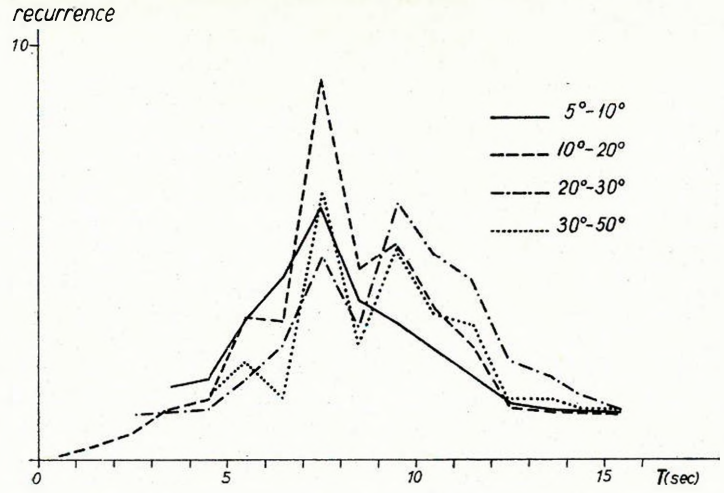

Fig. 21 Period-recurrence curves of 1000 coda-waves
21. ábra 1000 kóda-hullám periódusainak gyakorisági görbéje
Рис. 21. Кривая повторяемости периодов 1000 волн-код

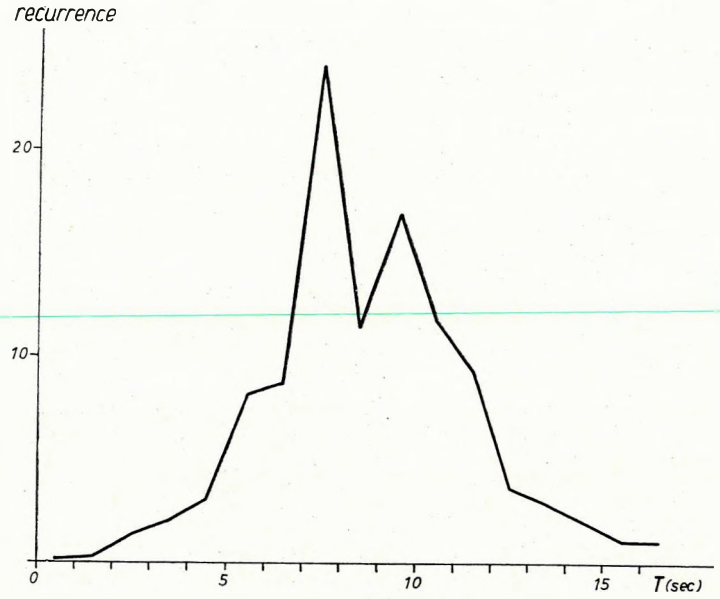

Fig. 22 Period-recurrence curves united
22. ábra A periódusgyakorisági görbék együttes ábrázolása
Рис. 22. Совместное представление кривых повторяемостей периодов

interrelation, the method of least squares was applied to the entire complex of data.

According to experiences gained in analysis of microseisms, one is entitled to assume that distance-dependence is quadratic and magnitude-dependence is linear. Consequently

$$T = a\Delta^{\circ 2} + b\Delta^{\circ} + cM + d. \tag{16}$$

Having used the 1000 data from the 5°—50° distance-interval to calculate the constants of (16), the equation

$$T = -0{,}0036\ \Delta^{\circ 2} + 0{,}23\ \Delta^{\circ} + 0{,}34\ M + 4{,}36 \tag{17}$$

has been obtained.

The quadratic part, however, is no more than a formal calculation, since the function has, at $\Delta^{\circ} = 32^{\circ}$, an extreme value. Explicitly, this means that T increases from zero to 32°, thereafter it decreases. This contradicts to actual experiences in the study of surface waves, thus it can easily be rejected. A linear smoothing was applied, omitting data of the 5°—10° interval, for this interval showed one peak only. Thus, 729 data have been left, but all of approximately identical recurrence. This way, the following equation was obtained

$$T = 0{,}042\ \Delta^{\circ} + 0{,}0016\ M + 8{,}46. \tag{18}$$

describing the properties of coda-waves from the 10°—50° interval better.

It was stated earlier (see Figs. 16, 17, 18) that *periods cannot depend considerably on distance.* Equ. (18) conveys the intelligence that periods, among

them the dominant one, are apt to shift; namely, the period 7—8 sec shifts toward 9—10 sec with increasing distance. The physical meaning of this phenomenon is that increasing distance gives a chance to absorption and to waves with a period-response characteristic for thicker units (layers). Putting it into an explicit form: in case of epicentral distances $0 < \Delta° < 5°$, low-period peaks (characteristic for near-surface layers), in case of e.d. $5° < \Delta° < 10°$, 7—8 sec peaks (characteristic for a complex of such a period-response), are obtained, in case of $10 < \Delta°$, higher period peaks (characteristic for a thick unit) dominate.

The fact that the coefficient of M is small, is of particular interest: it serves, namely, as another proof of the plate-vibration character of coda-waves. As it is well known, the pitch-level of a vibrating string or plate is independent of the amplitude of vibration, it depends only on the material, thickness and stress of the string or plate.

The smallness of the coefficient in question is remarkable anyway, for the period of body waves and surface waves is magnitude-dependent, as a rule. Thus the result obtained and explained so far, proves the origin of coda-waves to be different from theirs, and proves the coda-waves to be nearly insensitive to distance.

The next step of approach is to assume vibrations highly similar to Rayleigh-waves (HARDTWIG, 1962).

Regarding plane waves, the solutions of the wave-equation can thus be written

$$u = c\Gamma_1(\varkappa, z) \cos k(x - Vt)$$

$$w = c \frac{1 - \varkappa_0}{\sqrt{1 - 2\varkappa_0}} \Gamma_2(\varkappa, z) \sin k(x - Vt)$$

where

$$\Gamma_1(k, z) = e^{-q_1 z} - (1 - \varkappa_0) e^{-q_2 z}$$

$$\Gamma_2(k, z) = -(1 - \varkappa_0) e^{-q_1 z} + e^{-q_2 z}.$$

Substituting the solutions in the equations of condition, the following term is obtained:

$$3\varkappa_0^3 - 12\varkappa_0^2 + 14\varkappa_0 - 4 = 0.$$

The only solution which can be selected from this, is that which is smaller than the unit. Thus, the coefficient $\varkappa_0 = 1 - \frac{1}{\sqrt{3}} = 0{,}42265$. C, and parameters

$$q_1 = +\varkappa \sqrt{1 - 2/3 \cdot \varkappa_0} \qquad q_2 = +\varkappa \sqrt{1 - 2\varkappa_0}$$

jointly determine the attenuation of amplitudes with depth. The values of q_1 and q_2 are given by the following terms:

$$q_1 = \frac{2\pi}{\lambda} \cdot 0.8475 \qquad q_2 = \frac{2\pi}{\lambda} 0.3933$$

where λ is the wave-length.

It was mentioned above that codas don't originate from a point-source, not even from a linear-source. In fact, they have a source-area. Thus, velocity determination is rather uncertain. If accepting the velocity value $V=3{,}2$ km/sec observed in microseisms, the following values are obtained

$$q_1=\frac{2\pi\cdot 0.8475}{3{,}2}\cdot\frac{1}{T}=0.772\,\frac{1}{T},$$

$$q_2=\frac{2\pi\cdot 0.3933}{3{,}2}\cdot\frac{1}{T}=1.6640\,\frac{1}{T}.$$

Hence, longer periods are less attenuated with depth.

The amplitudes of u and w are

$$\eta=c\Gamma_1(k,z) \qquad\qquad \xi=c\,\frac{1-\varkappa_0}{\sqrt{1-2\varkappa_0}}\,\Gamma_2(k,z).$$

When determining constant c, the amplitude of horizontal displacement along the surface $z=0$ should be the unit.

$$1=c\Gamma_1(k,0)=C\varkappa_0; \qquad \text{hence, } c=\frac{1}{\varkappa_0}.$$

So, the amplitude of vertical displacement on the plane $z=0$ is 1,4679. This is quite natural, for in the process of particle-motion of Rayleigh-waves, the rate of major and minor axes of the ellipse is just the above value. Rayleigh-waves satisfying this consideration can, only in infinite half-space, arise. To turn the pattern into plate-model, it is necessary, after HARDTWIG, to assume a layer coupled to another underneath, but through a very thin intermediate layer, i.e. loosely. In this intermediate,—one might say transitional—layer, amplitudes are apt to decrease rapidly. Let two waves of periods T, resp. T', of vertical amplitudes Z, resp. Z' on the surface, change their amplitudes to ξ_0, resp. ξ_0' in depth Z_0.

Let us approach the nature of the decrease in the following manner:

$$\frac{Z}{n}=\frac{\xi}{\xi_0} \quad \text{and} \quad \frac{Z'}{n}=\frac{\xi'}{\xi_0'}.$$

Then

$$\frac{Z'}{Z}=\frac{\xi_0'}{\xi_0},$$

with earlier determined values:

$$z_0=\frac{TT'\ln\dfrac{Z'}{Z}}{(T'-T)0.772}. \tag{19}$$

Since period-recurrence curves showed identical peaks, it was easy to presume, that the period-values of the peak-range were in the above relation with the plate-thickness searched for.

To calculate Equ. (19) numerically, an amplitude vs. period graph is necessary. For this reason, only an abt. one fifth part of the data of Fig. 23 is

suitable. This curtailing is caused by the particle-motion of coda-waves. Only a part of the wave-pattern can be identified as Rayleigh-type waves, therefore only such waves of the vertical components were taken into consideration, where clear period-values were accompanied by rapid amplitude-change. The number of data: 182, but only their 50% satisfy the above condition, the other 50% have been selected at random.

Periods vs. amplitudes, smoothed with a quadratic curve (using the least squares method), gave the following formula:

$$T = -0{,}47\, Z^2 + 4{,}28\, Z + 1{,}83. \tag{20}$$

The T,T' and Z,Z' series, for the surroundings of the first recurrence-peak around 7—8 sec, are demonstrated (calculated with overlapping period-intervals) on Table I. The mean value of z_0 is 18,4 km.

Table II shows the same series for period-range around 9—10 sec. The mean value of z_0, in this range, is 29,63 km.

The round numbers: 7—8 and 9—10 sec are, actually, varying between 7,6 and 8,5, and 9,6—10,5 respectively. This fact may introduce some slight

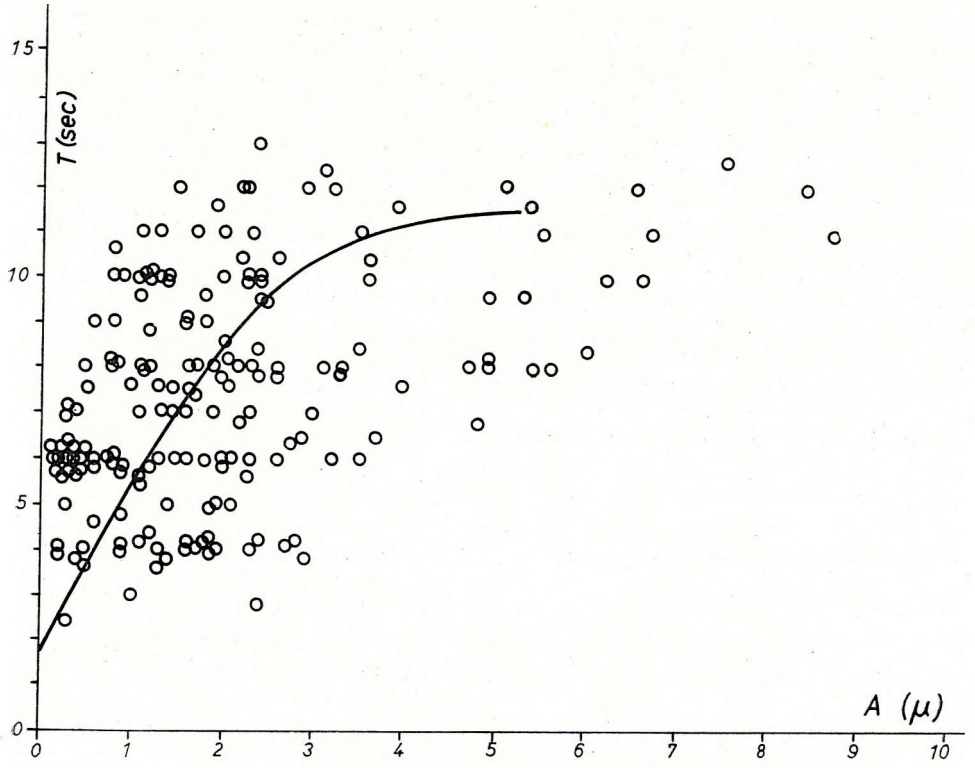

Fig. 23
23. ábra
Рис. 23.

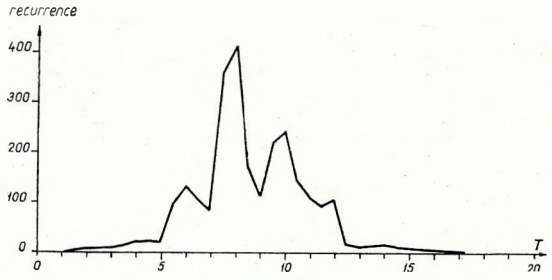

Fig. 24 Recurrence curve for overlapping period-intervals

24. ábra Az egymást fedő periódus-intervallumokra számított gyakorisági görbe

Рис. 24. Кривая повторяемости, расчитанная для перекрывающих друг друга интервалов периодов

calculational error, and is responsible for relatively large deviations on the tables.

The results of calculations with overlapping period-intervals is demonstrated on Fig. 24. Beside the two maxima mentioned, a weak maximum shows up between 5—7 sec, too. The corresponding depth is 13,7 km. Its significance doesn't even come near to that of the former ones, but it is thought to be worth of mentioning.

Table I.

T	T'	Z	Z'	Z_0
7,475	7,612	1,60	1,65	16,42
7,475	7,748	1,60	1,70	16,74
7,748	7,880	1,70	1,75	17,11
7,748	8,011	1,70	1,80	17,52
8,139	8,265	1,85	1,90	18,51
8,139	8,389	1,85	1,95	18,57
8,389	8,510	1,95	2,00	20,11
8,389	8,629	1,95	2,05	19,17
8,510	8,745	2,00	2,10	20,06
8,629	8,745	2,05	2,10	19,80

Table II.

T	T'	Z	Z'	Z_0
9,395	9,592	2,40	2,50	24,42
9,688	9,781	2,55	2,60	26,00
9,688	9,871	2,55	2,65	25,90
9,960	10,045	2,70	2,75	28,60
9,960	10,129	2,70	2,80	28,24
10,210	10,289	2,85	2,90	30,40
10,210	10,366	2,85	2,95	30,25
10,366	10,440	2,95	3,00	31,80
10,366	10,512	2,95	3,05	32,20
10,512	10,581	3,05	3,10	33,30
10,512	10,713	3,05	3,20	34,80

When sampling the records, coda-waves have arbitrarily been considered as Rayleigh-waves. In reality, however, codas must be composed of several kinds of surface waves. To extinguish any other components, first of all a vertical seismograph was, as mentioned, used. Secondly, for a special coda-analysis such an earthquake was selected, where the tangent of the great circle traversing the epicentre and the recording-station was E-W oriented, consequently Rayleigh-type waves could best be expected on the vertical and E-W component. The particle-motion, sampled from certain sections of the coda, is demonstrated on Fig. 25. Although no completely clear Rayleigh-ellipse could be expected, the overwhelming majority of the graphs show particlemotions approximating forward or backward rotating ellipses.

Not every wave of a complete coda, however, approximates the Rayleigh wave even to such an extent. Nevertheless, the amplitudes of all measurable waves (1000 data!) have been plotted against period (Fig. 26). The mass of data is very similar to the figure of KANAI et al. (1954) obtained for short-period microseisms. The only essential difference is that the bottom-dots on Fig. 26 show a decided thickening. It is interesting to note, how the coda-pattern reminds of that of microseisms.

Just for sure, the phenomenon was subjected to another test. To turn the dots into a quadratic function of period vs. amplitude, however, required some trick, for the "cloud" of dots was too scattered. It was assumed that to zero periods, zero amplitudes belong, and their number was equalled to the number of dots. The equation of the curve obtained in this way is:

$$T = -0{,}32\, z^2 + 4{,}13\, Z + 1{,}98.$$

Comparing this equation to the former one (the curve of which is likewise plotted on Fig. 26), the difference is, apparently, rather slight. The deviation, however, increases toward higher periods, and for good reasons: the first equation was based on systematically selected data, the second, on *every* data. In establishing the first equation, no high periods were needed, because the three peaks pre-selected the ranges of interest. It is obvious that the second curve was "pulled down" by the higher periods. The quadratic nature of the curve is likewise questionable, and the whole problem requires further investigations, moreover: it indicates a possible direction of research.

It has not been mentioned so far that the thickness-data, if regarded as referring to crustal structure (to the Conrad, and Moho surface, namely), are very close to those obtained by DSS (MITUCH—POSGAY, 1967/68). The value 29,63 km might symbolize the maximum thickness of the crust of the Carpathian Basin, for the crust of this region is a cupola-bottomed plane-concave slab (the least DSS thickness is abt. 23 km), for the station is situated on the margin of the basin. The value 18,4 km coincides, almost within the order of meters, with the DSS-determined Conrad depth. This might mean that the granitoid part of the crust is plane-parallel, contrarily to the entire crust.

Anyway, it seems to have been a successful endeavour, utilizing the period-recurrence and period vs. amplitude relation of coda-waves, to obtain data for crustal structure; data which are fairly supported by other results. The concept, consequently, must have been correct: the explanation of coda-waves by plate-vibrations is not irrealistic at all.

The only problem left, is the loose coupling. Many explanations can be,

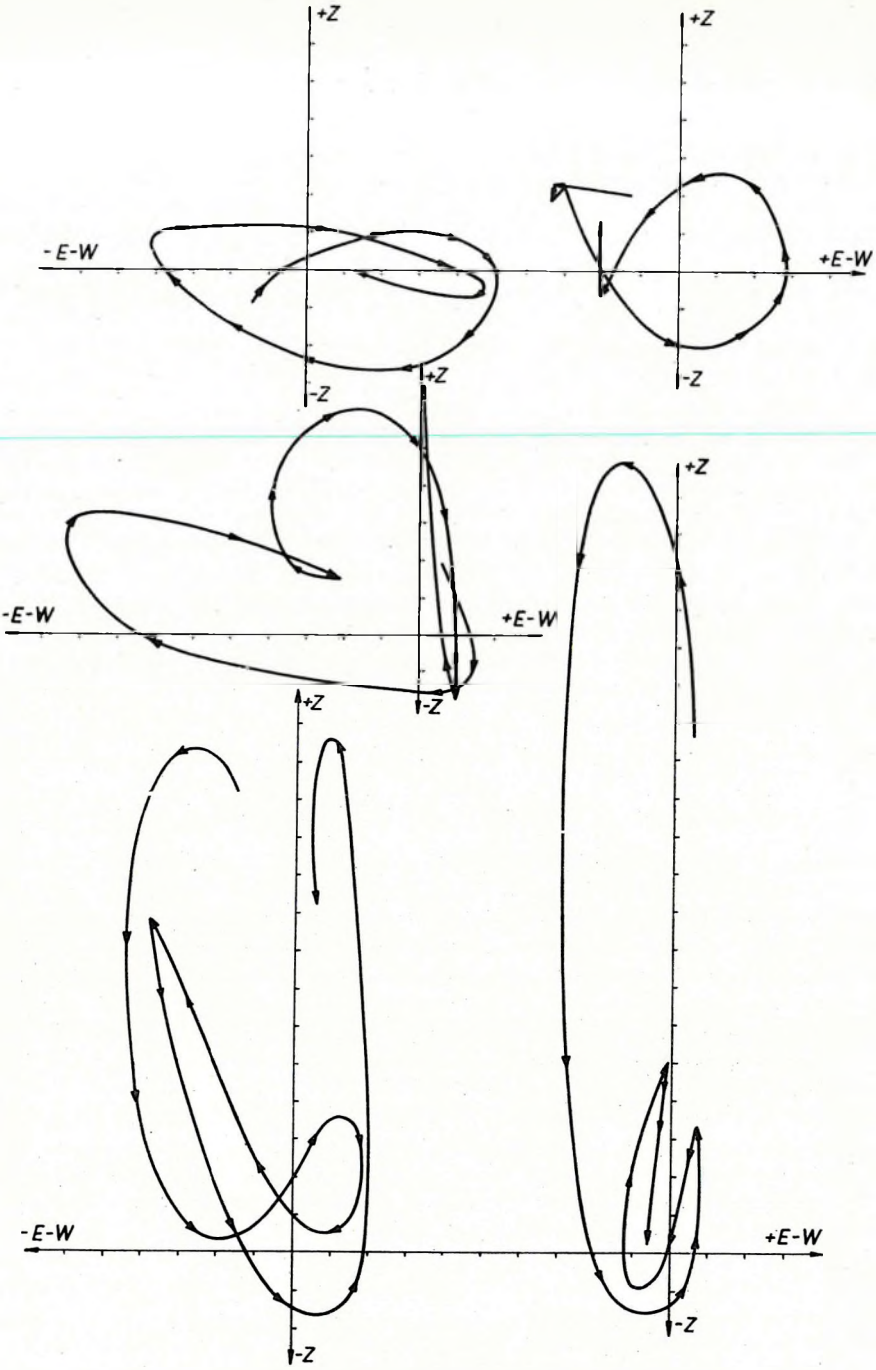

Fig. 25 Particle-motion of an earthquake of 25, 7 (22, 49, 41,3), 1969 $\varphi = 21{,}6$ N $\lambda = 111{,}9$ E $M = 5{,}4$

25. ábra 1969. VII. 25 22 49 41,3 $\varphi = 21{,}6$ N $\lambda = 111{,}9$ E, M = 5,4 rengés kóda-hullámainak részecskemozgása

Рис. 25. Смещение частиц волн-код землетрясения, происшедшего 25 VII 1969, 22 49 41,3, $\varphi = 21{,}6$ N, $\lambda = 111{,}9$ E, $M = 5{,}4$.

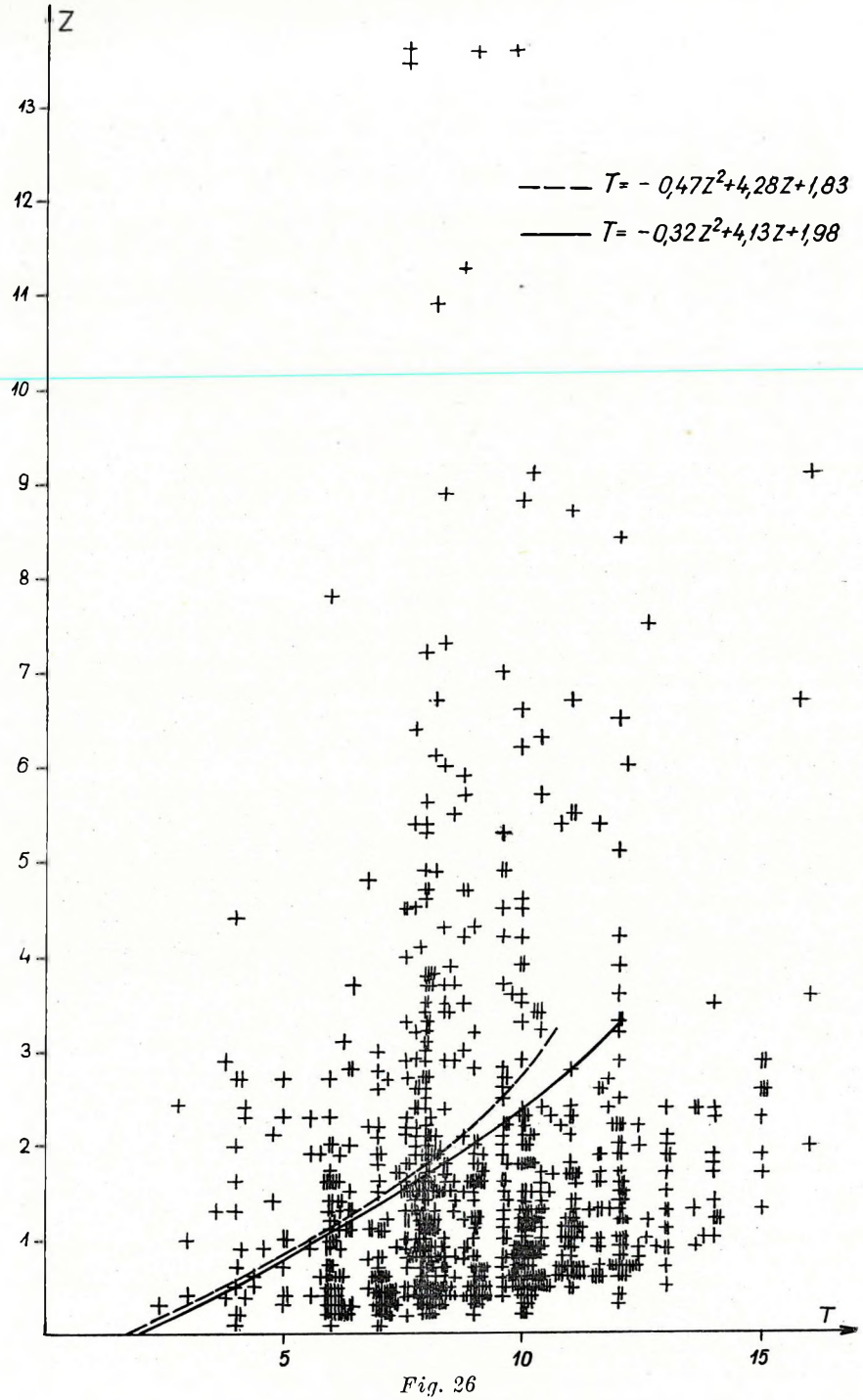

Fig. 26
26. ábra:
Рис. 26.

and actually have been advanced about the nature of the "intermediate layers" (e.g. MÜLLER—LANDISMAN, 1966). It is a matter of fact, that the clarification of this phenomenon requires a great deal of further investigations.

Anyway, if one accepts the loose coupling for a fact, the interpretation of Equ. (1a) will be easier at once.

In such a case, namely, the necessary considerations are rather simple and, besides, consistent with observed and reported facts. The pattern is as follows: the wide-band waves generated in the source-area of the epicenter, in great majority correspond in their period to the natural periods of the plates (layers, crustal layers) at hand, and travel forth as plate-vibrations. The absorption coefficient of surface waves is small, thus the energy-loss during the travel is likewise slight. Hence, it is easy to comprehend, why the duration of the surface waves (as described by Equ. [1a]) is not significantly depending on distance. During the travel, their dominant periods always correspond to the local structural properties (material, thickness) of the plate, i.e. to the periods depending on these properties. The data, in which the phenomenon reveals itself, albeit statistically random, are suitable to determine and to trace crustal structure traversed by these waves.

The possible ways of further investigations:

1. whether there is or there is not a recurrence-peak in the ultra-long period-range; if yes, perhaps it would be suitable to trace the depth-variation of the Gutenberg-channel, and what the correlation is between the depth-data obtained this way and by other means (e.g. MTS);

2. model-experiments should clarify such forms of coupling which allow quasi-free plate-vibrations;

3. consideration should be given to turning these investigations over to the applied field, namely, to test plate-thickness determinations in the near-surface layers (within the reach of geophysical exploration);

4. it is suggested to extend these investigations to regions, considerably differring from the Carpathian Basin; it is thought, namely, that paltform-regions, shields, especially with a thick station-network, are even more suitable for such investigations than the small, closed, unevenly thin-crusted Carpathian Basin.

These tasks, however, exceed the intention of the present paper.

LIST OF REFERENCES

AKI, K., 1969: Analysis of the seismic coda of local earthquakes as scattered waves. Journ. of Geophys. Res. 74. 2.

BISZTRICSÁNY, E., 1958a: A new method for the determination of earthquake magnitudes. Geofizikai Közl. (Geophysical Transactions) VII. 2.

BISZTRICSÁNY, E., 1958b: On the problem of magnitude determination. Zeitschrift f. Geophysik 24.

BISZTRICSÁNY, E., 1970: Investigations on the dispersion of the surface waves. Acta Geod. et Geoph. etc. (in press).

HARDTWIG, E., 1962: Theorien zur mikroseismischen Bodenunruhe. Akademische Verlagsgesellschaft, Leipzig.

HASKELL, N. A., 1953: The dispersion of surface waves on multilayered media. B.S.S.A. pp. 17—34.

HEALY, J. H.—PRESS, F., 1960: Two dimensional seismic models with continuously variable velocity depth and density functions. Geophysics, 25. 5.

KANAI, K.—TANAKA, T.—OSADA, K., 1954: Measurement of the micro-tremor. Bull. Earthqu. Res. Inst., Tokyo, XXXII. Part. 2.
LAMB, H., 1917: On elastic waves in a plate. Proc. Roy. Soc., London.
MITUCH E.—POSGAY K., 1967/68: Die Ergebnisse der seismischen Messungen, ausgeführt an den ungarischen Abschnitten der internationalen Erdkrustenforschungsprofile. Zavod Geoloska i Geofizička Istrazivanja. Serija C. Bulletin VIII/IX. Beograd.
MÜLLER, ST.—LANDISMAN, M., 1966: Seismic studies of the Earth's crust in continents; Part I. Evidence for a low-velocity zone in the upper part of the lithosphere. Geophys. Journ. R.A.S. 10. 525—538.
SOLOVIEV, S. L., 1965: Seismicity of Sakhalin. Bull. Earthqu. Res. Inst., Tokyo, 43.
TSUMURA, K., 1967: Determination of earthquake magnitude from total duration of oscillation. Bull. Earthqu. Res. Inst., Tokyo.
WIECHERT, E.—ZOEPPRITZ, A. K., 1907: Über Erdbebenwellen. Nachr. Ges. Wiss. Göttingen, Math. Phys.

TARTALOM

GEOPHYSICAL TRANSACTIONS VOL. XIX. 1969

СОДЕРЖЕНИЕ